Experimental Investigation of Influence of SOA-Induced Nonlinear Distortion on High-Symbol-Rate 168-GBaud Signal for Achieving Ultra-Broadband Optical Frontend

F. Hamaoka[(1)], M. Nakamura[(1)], T. Kobayashi[(1)], M. Nagatani[(1, 2)], H. Wakita[(2)], H. Yamazaki[(1, 2)], Y. Ogiso[(2, 3)], and Y. Miyamoto[(1)]

(1) NTT Network Innovation Laboratories, NTT Corporation, 1-1 Hikari-no-oka, Yokosuka, Kanagawa, 239–0847 Japan
(2) NTT Device Technology Laboratories, NTT Corporation, 3-1 Morinosato-Wakamiya, Atsugi, Kanagawa, 243–0198 Japan
(3) NTT Device Innovation Center, NTT Corporation, 3-1 Morinosato-Wakamiya, Atsugi, Kanagawa, 243–0198 Japan
fukutaro.hamaoka.xz@hco.ntt.co.jp

Abstract: We propose a transmitter configuration using an ultra-broadband optical frontend integrated with a bandwidth multiplexer and SOA. Experiments demonstrate the SOA-induced nonlinear distortion slightly affects (<1-dB SNR degradation) the 1-Tb/s 168-GBaud signal using AMUX-integrated frontend. © 2022 The Author(s)

1. Introduction

In optical transmission systems, the capacities have been growing continuously alongside breakthrough technologies such as wavelength-division multiplexing (WDM) transmission with erbium-doped fiber amplifiers (EDFAs) and digital coherent transceivers. With the increased capacity of these systems, a small form factor, such as the integrated coherent transmit-receiver optical subassembly (IC-TROSA) [1], is required to reduce the power consumption of coherent transceivers with high capacity per wavelength. The semiconductor optical amplifier (SOA) is a key component in integrated coherent transceivers due to its small size and low power consumption. An IC-TROSA configuration including SOAs as a transmitter booster and receiver pre-amplifier has been reported for 400- to 600-Gb/s applications with 64-GBaud 16 quadrature amplitude modulation (QAM) and 64QAM signals [2]. In addition, as SOAs have high design flexibility for the amplification band, they have also recently been used in digital coherent experiments for 100-nm ultra-wideband WDM transmission [3].

For further increasing the signal capacity per wavelength, >100- to 200-GBaud-class high-symbol-rate signal handling technologies that electrically multiplex the pre-processed signal from the sub digital-to-analog converters (DACs) in a transmitter-side (Tx) digital signal processing (DSP) have been proposed (e.g., [4–6], which overcome the bandwidth limitation of complementary metal-oxide-semiconductor (CMOS) DACs). We have previously developed an analog multiplexer (AMUX) integrated optical frontend that can double the symbol rate without increasing the interconnection bandwidth between a Tx-DSP and the frontend [7]. In this study, we propose a transmitter configuration with a Tx-DSP and an ultra-broadband optical frontend consisting of a bandwidth multiplexing function and an SOA to achieve a high-performance digital-coherent transmitter. We also experimentally demonstrate the influence of the SOA-induced nonlinear distortion on a high-symbol-rate 168-GBaud signal to achieve the proposed high-symbol-rate transmitter.

2. High-Symbol-Rate Transmitter Configuration with Ultra-Broadband Optical Frontend

Figure 1(a) shows the AMUX-integrated optical frontend with driver amplifiers and an in-phase and quadrature modulator (IQM) we recently developed using our indium phosphide (InP) technology [7]. Usually, the increase of

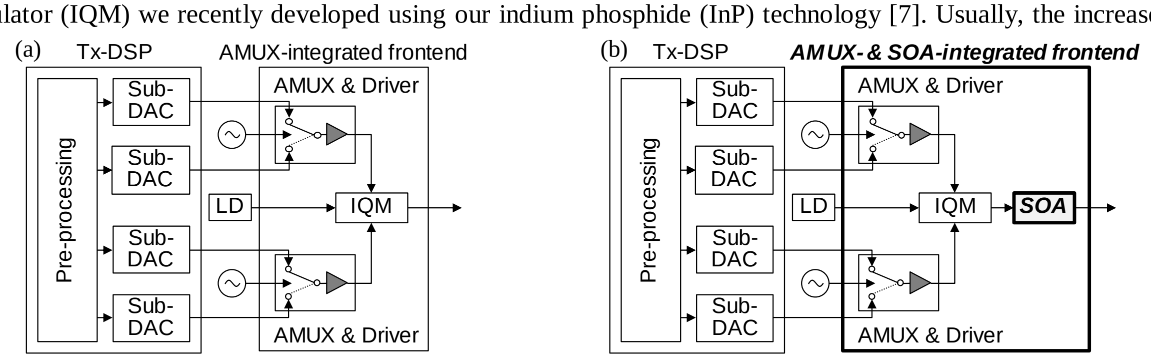

Fig. 1. High-symbol-rate transmitter: (a) conventional configuration and (b) proposed configuration with ultra-broadband optical frontend integrated with bandwidth multiplexing function (AMUX) and SOA.

the symbol rate is limited by the bandwidth of CMOS-DACs and the high-speed signal module interconnection among DACs, driver amplifiers, and an IQM using coaxial cables. The AMUX-integrated architecture shown in Fig. 1(a) can overcome this limitation and double the symbol rate without increasing the interconnection speed between the Tx-DSP and the frontend. In this study, as shown in Fig. 1(b), we propose a transmitter configuration with Tx-DSP and an ultra-broadband optical frontend consisting of AMUXs, driver amplifiers, an IQ modulator, and an SOA. The key advantage of the proposed configuration is that the frontend integrates the SOA as a pre-amplifier to improve the output optical power of the high-symbol-rate signals from the frontend while simultaneously enabling small size integration and low power consumption. Also, the high-symbol-rate transmitter with the bandwidth multiplexing function by AMUX can double the symbol rate with the narrow bandwidth interconnection between the Tx-DSP and the integrated optical frontend.

3. Experimental Setup

Since the carrier lifetime in an SOA is almost on the same order as the symbol rate (several tens of Giga Bauds) in coherent transceivers, SOA-induced nonlinear distortion by the signal pattern effect occurs and degrades the signal characteristics. However, to the best of our knowledge, the influence of the SOA-induced nonlinear distortion on the high-symbol-rate signal is unknown for the symbol rate of >100 GBaud. Therefore, we conducted experiments to evaluate the high-symbol-rate signal performance in a back-to-back condition while amplifying the signal by an SOA for a 168-GBaud polarization division multiplexed (PDM) probabilistic constellation shaped (PCS) 16QAM signal generated with our previously developed AMUX-integrated frontend [7]. Figure 2 shows the experimental setup.

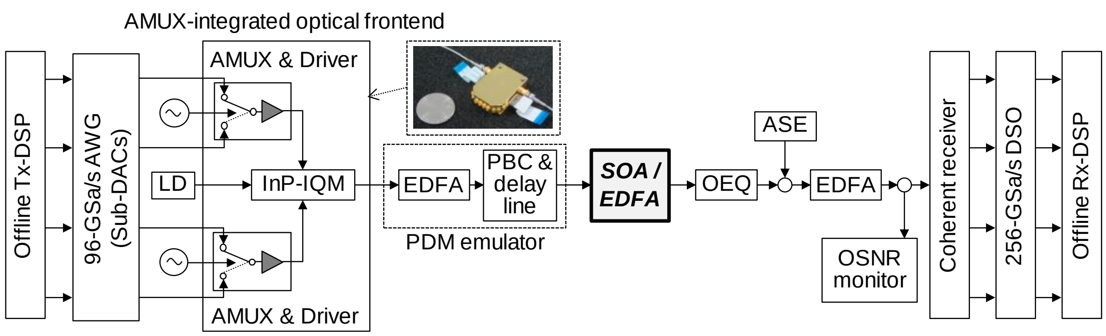

Fig. 2. Experimental setup to investigate characteristics of 42-, 64-, and 168-GBaud PDM PCS-16QAM signals amplified by SOA.

In the offline Tx-DSP, an extended probabilistic amplitude shaping with a constant composition distribution matcher [8] converted a bit sequence derived from the Mersenne Twister into PCS-16QAM with the entropy of 3.739 bits based on a discrete Maxwell Boltzmann distribution. In the PCS-16QAM symbols, we assume 1.64% pilot symbols for the offline receiver-side (Rx) DSP. The roll-off factor of the root-raised cosine filter was 0.01 for the Nyquist-shaped signal. The symbol rates of the PCS-16QAM signals were 42, 84, and 168 GBaud. Digital pre-emphasis was then applied to the signals to compensate for the frequency response and the in-band crosstalk in the AMUXs. The transmitted signal was pre-processed in a format specified by the digital-preprocessed analog-multiplexed DAC (DP-AM-DAC) scheme [9]. The pre-processed low-speed signals, from a four-channel arbitrary waveform generator (AWG) operating as sub-DACs at a sampling rate of 96 GSa/s with an analog bandwidth of 32 GHz, were input to an AMUX-integrated optical frontend with a 6-dB analog bandwidth of 80 GHz that consisted of AMUXs, driver amplifiers, and an IQM based on in-house InP technology [7]. The operating clock frequency of the AMUXs was 42 GHz. The signal was modulated by InP-IQM with a carrier frequency of 193.735 THz in the C band. The PMD signal was generated by using a PDM emulator consisting of an EDFA, a polarization beam combiner (PBC), and a delay line. As shown in Fig. 2, the PDM signal was then amplified by an SOA and an EDFA that were alternately switched to determine how the SOA-induced nonlinear distortion affected the signal characteristics. An optical equalizer (OEQ) using a flexible grid wavelength selective switch was applied to the PDM signal to compensate for the frequency response by a joint digital-and-optical equalization scheme to reduce the peak-to-average power ratio of the pre-processed signals from the sub-DACs [10]. An amplified spontaneous emission (ASE) noise was added to the signal to examine the influence of only the SOA-induced nonlinear distortion on the signal. The optical signal-to-noise ratios (OSNRs) of the signal were monitored after the signal was amplified by the receiver-side EDFA.

The signal was received by a coherent receiver consisting of an optical local oscillator (LO) with a frequency of 193.735 THz, an optical hybrid, and four 100-GHz balanced photodiodes. After digitizing the signal received at a four-channel 110-GHz digital storage oscilloscope at a sampling rate of 256 GSa/s, the signal was demodulated by the offline Rx-DSP [10]. Finally, we measured the SNR and normalized generalized mutual information (NGMI) [11] to evaluate the signal characteristics in the back-to-back configuration. The net rate of the 168-GBaud PDM PCS-16QAM signal was 1 Tb/s [= 2 × {3.739 – (1 – 0.826) × 4} / 1.0164 × 168 Gbaud], assuming a forward error correction (FEC) code with a 20.94% overhead corresponding to a code rate of 0.826 [12]. At the same configuration, the net rates of the 42- and 84-GBaud PDM PCS-16QAM signals were respectively 0.25 and 0.5 Tb/s.

4. Results and Discussion

We experimentally investigated the influence of the SOA-induced nonlinear distortion on the 42-, 84-, and 168-GBaud PDM PCS-16QAM signals and discuss the results in this section. The OSNR of the signals was set to 17, 20, and 23 dB by adding the ASE noise for the symbol rates of 42, 84, and 168 GBaud, respectively, so that the SNRs of the received signals were the same and we could observe only the influence of the SOA-induced nonlinear distortion on the signal quality. The optical input power to the SOA was 0 dBm. Figure 3(a) shows that the SOA gain increased with increasing the injection current. The SNR penalty from the SNR difference between the signals amplified by the EDFA and the SOA is shown in Fig. 3(b) as a function of the injection current of the SOA. In the case of the symbol rate at 42 and 84 GBaud, the SNR penalty got significantly worse, as indicated by the SOA-induced nonlinear distortion observed on the signal constellations (as seen in Fig. 3(c)) with increasing the injection current (i.e., with increasing the SOA gain). On the other hand, as shown in Fig. 3(b) and (c), the SNR penalty of the 168-GBaud signal was 0.96 dB, which is smaller by 2 and 1 dB than those of the 42- and 84-GBaud signals at the injection current of 350 mA with reducing the effect of the SOA-induced nonlinear distortion on the 168-GBaud signal. The qualities of the signals amplified by SOA and EDFA were almost identical, especially at the current of 100 mA. The SOA-induced nonlinear distortion had hardly any effect on the 168-GBaud signal in this case. As shown in Fig. 3(d), the NGMIs of the 168-GBaud PDM PCS-16QAM signal at all the injection currents were better than the NGMI limit of 0.857 [12] as compared to those of the 42-, and 84-Gbaud signals due to the significant reduction of the SOA-induced nonlinear distortion. These results demonstrate that the proposed transceiver configuration with ultra-broadband optical frontend including the SOA can achieve the net rate 1-Tb/s 168-GBaud PDM PCS-16QAM signal generation with a high-gain optical output.

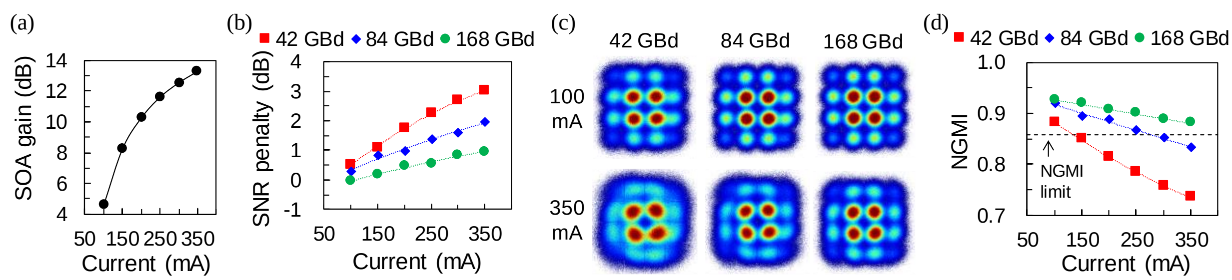

Fig. 3. Experimental results: (a) SOA gain, (b) SNR penalty as a function of injection current of SOA, (c) signal constellations, and (d) NGMI as a function of injection current of SOA. The SNR penalty was the SNR difference between the signals amplified by the EDFA and the SOA.

5. Conclusion

A high-symbol-rate digital coherent transmitter configuration with a TX-DSP and an ultra-broadband optical frontend consisting of analog multiplexers (AMUXs), driver amplifiers, an IQ modulator, and an SOA as a pre-amplifier was proposed to reduce the size and power consumption of the transmitter, which can double the symbol rate with the narrow bandwidth interconnection between the Tx-DSP and the frontend. We experimentally demonstrated that the SOA-induced nonlinear distortion slightly affected the 1-Tb/s 168-GBuad PDM PCS-16QAM signal quality with an SNR degradation of less than 1 dB compared with the case of EDFA. These results imply that SOAs can be integrated into an ultra-broadband optical frontend with the function of high-gain optical output for future ultra-high-symbol-rate transceivers.

References

[1] "Implementation Agreement for Integrated Coherent Transmit-Receive Optical Sub Assembly," OIF-IC-TROSA-01.0, Aug. 20, 2019.
[2] J. Zhou, *et al.*, *OFC2019*, Tu2H.7.
[3] J. Renaudier, *et al.*, ECOC2017, Th.PDP.A.3.
[4] H. Yamazaki, *et al.*, ECOC2015, PDP.2.2.
[5] X. Chen, *et al.*, OFC2016, Th5C.5.
[6] F. Hamaoka, *et al.*, Electron Lett, 54 (24), 1390 (2018).
[7] M. Nakamura, *et al.*, OFC2019, Th4B.4.
[8] G. Böcherer, et al., IEEE Trans. Commun., 63 (12), 4651 (2015).
[9] H. Yamazaki, *et al.*, J. Lightwave Technol., 35 (7), 1300 (2017).
[10] F. Hamaoka, *et al.*, ECOC2019, W4B.2.
[11] J. Cho, *et al.*, ECOC2017, M.2.D.2.
[12] M. Nakamura, *et al.*, ECOC2018, We3G.5.